Domain-wall energies and magnetization of the two-dimensional random-bond Ising model

C. Amoruso and A. K. Hartmann
Institut für Theoretische Physik, Universität Göttingen, Tammannstrasse 1, 37077 Göttingen, Germany
(Received 23 January 2004; published 29 October 2004)

We study ground-state properties of the two-dimensional random-bond Ising model with couplings having a concentration $p \in [0,1]$ of antiferromagnetic and $(1-p)$ of ferromagnetic bonds. We apply an exact matching algorithm which enables us the study of systems with linear dimension L up to 700. We study the behavior of the domain-wall energies and of the magnetization. We find that the paramagnet-ferromagnet transition occurs at $p_c \sim 0.103$ compared to the concentration $p_n \sim 0.109$ at the Nishimori point, which means that the phase diagram of the model exhibits a re-entrance. Furthermore, we find no indications for an (intermediate) spin-glass ordering at finite temperature.

DOI: 10.1103/PhysRevB.70.134425 PACS number(s): 75.10.Nr, 75.40.Mg

I. INTRODUCTION

Despite more than two decades of intensive research, many properties of spin glasses,[1] especially in finite dimensions, are still not well understood. For two-dimensional Ising spin glasses it is now widely accepted that no ordered phase for finite temperatures exists.[2–6] Furthermore, it seems clear that the behavior can be described well by a zero-temperature droplet scaling approach,[7–10] but one needs quite large system sizes to observe[11] the true behavior. One unanswered question is whether an additional phase, usually called *random antiphase*, exists[12–15] for $T \neq 0$ in two dimensions with an asymmetric distribution of random bonds. Also it is no clear whether at low temperatures the phase boundary of the ferromagnetic phase is perpendicular[16,17] to the p axis, p denoting the concentration of the antiferromagnetic bonds. The aim of the present paper is to reinvestigate this issues by studying the domain-wall energy and magnetization at zero temperature via the determination of *exact* ground states[18] for large system sizes and huge sample numbers. This allows us to draw much more reliable conclusions in comparison to past studies, where only considerable smaller system sizes could be studied.

The organization of the paper is as follows: In Sec. II, we will expose the model and briefly describe the polynomial matching algorithm, which allows us to treat large system sizes. Section III presents our results for the domain-wall energy. In Sec. IV, we explain the additional methods used to obtain the magnetization and show the results. Finally, we summarize and draw our conclusions in Sec. V.

II. THE MODEL AND THE METHOD

The model consists of $N=L^2$ spins $S_i = \pm 1$ on a simple square lattice with periodic boundary conditions in the x direction and free boundary conditions in the y direction. The Hamiltonian is

$$H = -\sum_{\langle ij \rangle} J_{ij} S_i S_j, \tag{1}$$

where the sum runs over all pairs of nearest neighbors $\langle ij \rangle$ and the J_{ij} are the quenched random spin-spin couplings. The couplings are set independently antiferromagnetic $(J_{ij}=-1)$ with a probability $p \in [0,1]$ and ferromagnetic $(J_{ij}=+1)$ with probability $(1-p)$.

The phase diagram of the model as a function of temperature T and the concentration p is shown in Fig. 1. The pure system $(p=0)$ has a transition at a Curie temperature $T_0 = 2[\ln(1+\sqrt{2})]^{-1}$, above which the system is paramagnetic. When antiferromagnetic bonds are introduced $(p>0)$, the ferromagnetic phase is destroyed at a threshold concentration $p_c(T)$. A particular curve on the $p-T$ plane is known as the Nishimori line[19] (NL). It is defined by the equation $\exp 2\beta = (1-p)/p$. On this line the internal energy is analytic and the spin-spin correlation functions obey the equalities $\langle \sigma_i \sigma_j \rangle^{2k-1} = \langle \sigma_i \sigma_j \rangle^{2k}$, for integer k. It was also proven[20] that a multicritical point delimiting two critical behaviors on the ferropara boundary coincides with the intersection of the NL with the boundary: this defines the Nishimori point (NP). Besides, by studying domain-wall energies of exact ground states for system's sizes up to $L=32$, Kawashima and Rieger[15] found that the stability of the ferromagnetic and spin-glass order cease to exist at a unique concentration for the antiferromagnetic bonds, so they concluded that there is no intermediate spin-glass phase.

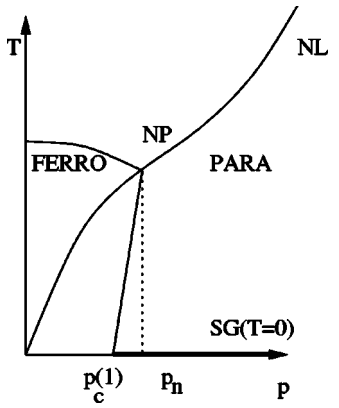

FIG. 1. The phase diagram of the two-dimensional random-bond Ising model, with the concentration p of antiferromagnetic bond and the temperature T on the vertical axis. It has been conjectured that the phase boundary from the NP falls vertically to the p-axis.

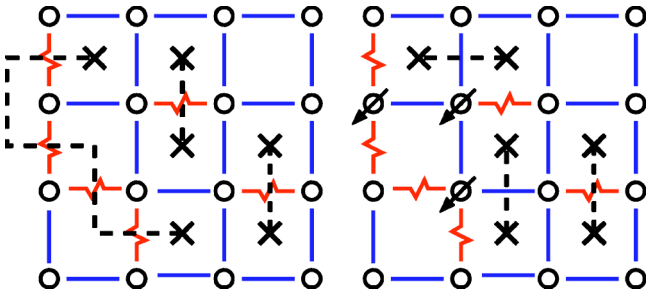

FIG. 2. 2d spin glass with all spins up (left, up spins not shown). Straight lines are ferromagnetic, jagged lines antiferromagnetic bonds. The dotted lines connect frustrated plaquettes (crosses). The bonds crossed by the dotted lines are unsatisfied. In the right part the GS with three spins pointing down (all other up) is shown, corresponding to a minimum number of unsatisfied bonds.

In this paper we want to compute numerically with high accuracy the critical concentration $p_c^{(1)}=p_c(T=0)$ corresponding to the para-ferro transition at zero temperature, and to compare this result with the believed value of the Nishimori point $p_n=0.109(1)$.[21,22] Furthermore, we want to check with high accuracy, whether there is an intermediate spin-glass phase at nonzero temperature.

We can reach a much higher precision compared to previous studies, by applying a matching algorithm. This allows to compute exact ground states for large system sizes, $N=700^2$ spins in our case. Let us now explain just the basic idea of the matching algorithm, for the details, see Refs. 23–25. The method works for spin glasses which are planar graphs, this is the reason, why we apply periodic boundary conditions only in one direction. In the left part of Fig. 2 a small $2d$ system with open boundary conditions is shown. All spins are assumed to be "up," hence all antiferromagnetic bonds are not satisfied. If one draws a dotted line perpendicular to all unsatisfied bonds, one ends up with the situation shown in the figure: all dotted lines start or end at frustrated plaquettes and each frustrated plaquette is connected to exactly one other frustrated plaquette. Each pair of plaquettes is then said to be *matched*. Now, one can consider the frustrated plaquettes as the vertices and all possible pairs of connections as the edges of a (dual) graph. The dotted lines are selected from the edges connecting the vertices and called a *perfect* matching, since *all* plaquettes are matched. One can assign weights to the edges in the dual graph, the weights are equal to the sum of the absolute values of the bonds crossed by the dotted lines. The weight Λ of the matching is defined as the sum of the weights of the edges contained in the matching. As we have seen, Λ measures the broken bonds, hence, the energy of the configuration is given by $E=-\Sigma_{\langle i,j\rangle}|J_{ij}|+2\Lambda$. Note that this holds for *any* configuration of the spins, since a corresponding matching always exists. Obtaining a ground state means minimizing the total weight of the broken bonds (see right panel of Fig. 2), so one is looking for a *minimum-weight perfect matching*. This problem is solvable in polynomial time.

The algorithms for minimum-weight perfect matchings[26,27] are among the most complicated algorithms for polynomial problems. Fortunately the LEDA library offers a very efficient implementation,[28] except that it consumes a lot of memory, which limits in our case the size of the systems to about $N=700^2$ on a typical 500 MB workstation.

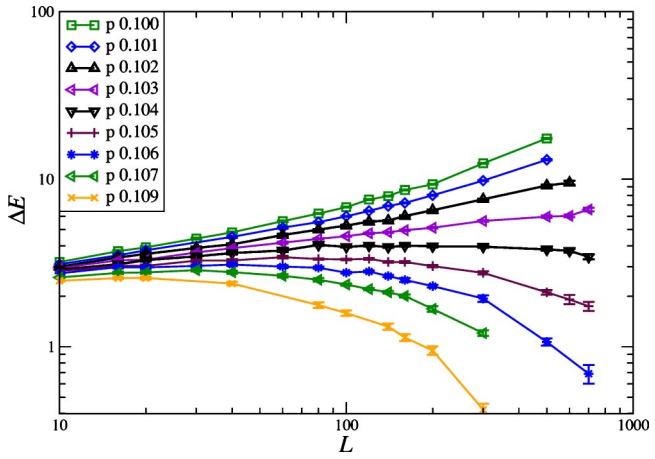

FIG. 3. The domain-wall energy ΔE of the random-bond model plotted as a function of the system size L for various ferromagnetic-bond concentrations p.

III. DOMAIN-WALL ENERGIES AND FINITE-SIZE SCALING

We calculate the domain-wall energy δE defined by $\delta E \equiv E_p - E_a$, where E_p and E_a are the ground-state energies with periodic and the antiperiodic boundary conditions in the x-direction, respectively. We take an average over the disorder. We are interested in the exponents ρ and θ_S that characterize the system-size dependence of the mean ΔE and the width $\sigma(\delta E)$ of the distribution of the domain-wall energies:

$$\Delta E \propto L^{\rho} \quad \text{and} \quad \sigma(\delta E) \propto L^{\theta_S}. \tag{2}$$

For a general dimensions d of the system, a positive value of ρ indicates the stability of a ferromagnetic phase For $\rho<0$,

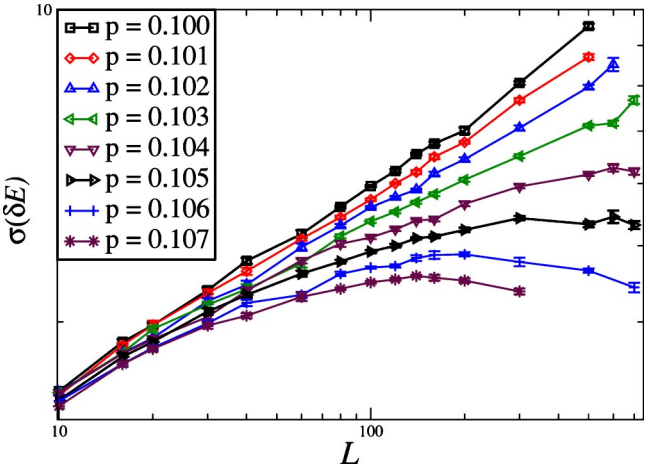

FIG. 4. The width of the distribution of the domain-wall energy $\sigma(\delta E)$ of the random-bond model plotted as a function of the system size L for various ferromagnetic-bond concentration p.

no ferromagnetic ordering is present. Then, in dimension d above the lower critical dimension d_c, we have $\theta_S > 0$ and spin glass-ordering is stable against thermal fluctuations. On the other hand, when $\theta_S < 0$, thermal fluctuations prevent spin-glass ordering.[10] The current belief is that in $d=2$, $\theta_S < 0$ holds for all concentrations $p_c^{(1)} < p < 1 - p_c^{(1)}$.

We have computed $\sigma(\delta E)$ and ΔE for sizes up to $L = 700$ and for values of p ranging from 0.100 to 0.109. We performed a disorder average of a number of realizations ranging from 30000 for the smallest sizes to typically 2000 for the largest size $L=700$. In Figs. 3 and 4 the mean and the width of the distribution of domain-wall energies are plotted as a function of the system size. We denote by $p_c^{(1)}$ and $p_c^{(2)}$ the critical concentrations of antiferromagnetic bonds at which the asymptotic L dependencies of ΔE and $\sigma(\delta E)$, respectively, change from increasing to decreasing, i.e., the concentrations where a ferromagnetic phase and a spin-glass phase, respectively, cease to exist at finite temperature. We conclude from the figures that $p_c^{(1)} \sim 0.103$, while for $p_c^{(2)}$ the "transition" is less sharp but the value is between 0.103 and 0.105. For small sizes, the width even seems to increase for all values of $p \in [0.1, 0.107]$ we have considered. For small sizes, at intermediate concentrations $p \in [0.1, 0.15]$, the mean of the domain-wall energy already decreases with system size, while the width of the distribution first increases, which appears as if the system exhibits some kind of spin-glass phase. This is probably the reason that in some previous studies[12–14] the existence of an additional intermediate phase has been assumed. We see that we have to consider large system sizes to observe the true behavior.

Another way to compute $p_c^{(1)/(2)}$ is to check the scaling relations for ΔE and $\sigma(\delta E)$ proposed in Ref. 15

$$\Delta E L^{\psi_1} = f_1((p - p_c^{(1)}) L^{\phi_1}), \tag{3}$$

$$\sigma(\delta E) L^{\psi_2} = f_2((p - p_c^{(2)}) L^{\phi_2}). \tag{4}$$

The parameters p_c, ϕ, and ψ for both moments of domain wall energies have to be chosen such that a good data collapse for all data is obtained. To quantify the "goodness" of this fit, we used an appropriate cost function $S(p_c, \phi, \psi)$ introduced in Ref. 29 whose minimum value should be close to unity when the fit is statistically acceptable. To minimize $S(p_c, \phi, \psi)$ we used the implementation of the simplex method offered by Numerical Recipes library.[30] The best fits give the estimates

$$p_c^{(1)} = 0.103(1) \quad \phi_1 = 0.75(5), \quad \psi_1 = -0.12(5) \tag{5}$$

with $S = 0.75$ and

$$p_c^{(2)} = 0.104(2), \quad \phi_2 = 0.74(5), \quad \psi_2 = -0.13(5) \tag{6}$$

with $S = 0.65$. The resulting scaling plots are shown in Figs. 5 and 6. We have estimated the error bars given above in the following way. For each parameter, we fix it to different values and perform the minimization over the remaining two parameters. In Fig. 7 we show as example a plot of this partly minimized value of $S(p_c, \psi, \phi)$ as a function of p_c. Our error bars are the ranges of values where $S(p_c, \psi, \phi)$ increases to twice of its minimum value.

Within the statistical errors the critical parameters for both moment of δE agree: this strongly suggest the absence of a spin-glass phase. Therefore there is a discrepancy between

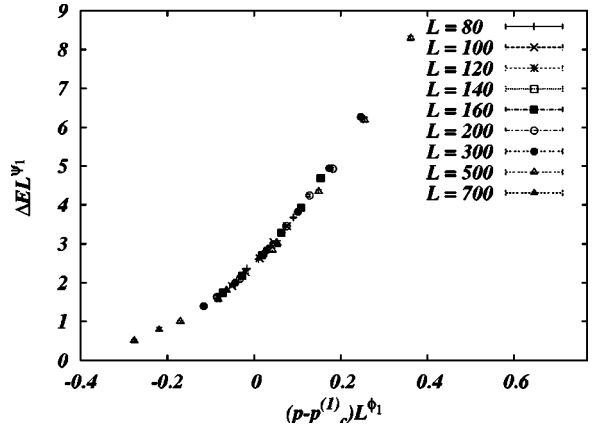

FIG. 5. The scaling plot of mean domain-wall energy ΔE versus the concentration of the antiferromagnetic bonds, using the values $p_c^{(1)} = 0.103$, $\phi_1 = 0.75$, $\psi_1 = -0.12$.

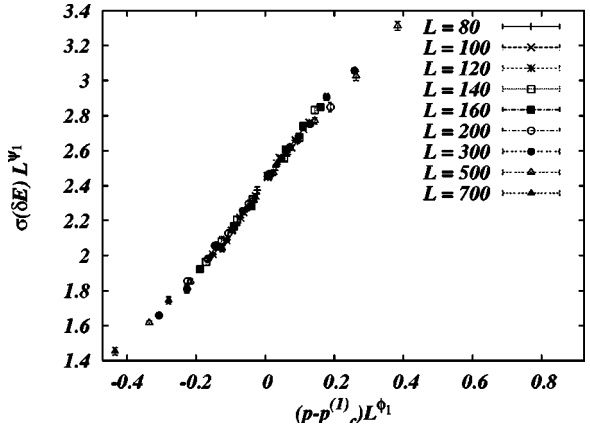

FIG. 6. The scaling plot of $\sigma(\delta E)$ versus the concentration of the antiferromagnetic bonds, using the values $p_c^{(2)} = 0.104$, $\phi_2 = 0.74$, $\psi_2 = -0.13$.

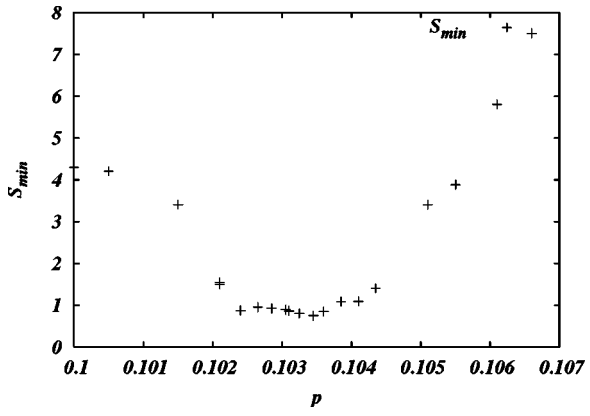

FIG. 7. Plot of the minimum value of $S(p_c, \psi, \phi)$ for different fixed values of p_c.

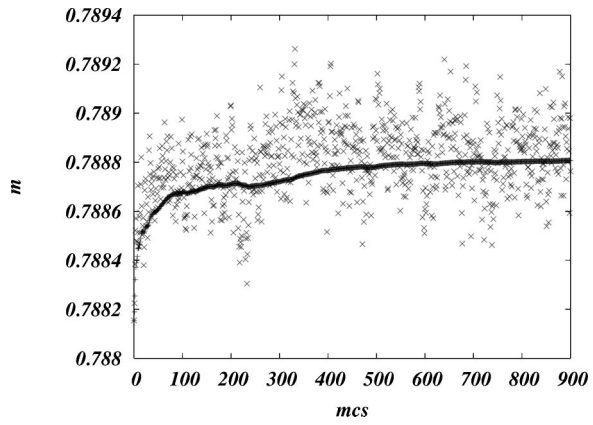

FIG. 8. Magnetization averaged over 100 samples ($L=300$, $p=0.1$) as a function of the number of MC steps for a zero-temperature single-spin-flip dynamics. The bold line is the running average (averaged over the samples).

the critical concentration p evaluated at the NP and at zero temperature, in disagreement with the conjecture $p_n=p_c^{(1)}$ by Nishimori[16] and later by Kitatani.[17] Later, Le Doussal and Harris[20] have shown that the tangent to the phase boundary at the NP is vertical. But this result does not exclude the possibility of a re-entrance in the phase diagram as shown in Fig. 1.

IV. STUDY OF THE MAGNETIZATION

We furthermore study the para-ferro transition by evaluating the magnetization and using the Binder cumulant crossing method.[31,32] The Binder cumulant is given by

$$B(p,L)=\frac{3}{2}\left(1-\frac{\langle m\rangle^4}{3\langle m^2\rangle^2}\right), \tag{7}$$

where $m=1/N\Sigma S_i$ is the magnetization and $\langle\cdots\rangle$ denotes the average over the disorder. For second order phase transitions, the curves for different sizes intersect at one point, the critical concentration $p_c^{(1)}$. This is a consequence of finite-size scaling.

The problem one has to face when studying system with discrete interactions, is the exponentially large number of states all giving the same energy. Hence there is no unique ground-state magnetization. For a given set of bonds we here determine one exact ground state using an efficient polynomial time "matching" algorithm, but we are not able to enumerate all the ground states.[33]

In order to check if "typical" configurations with respect to the magnetization are found, we first performed a zero-temperature Monte Carlo (MC) simulation which consists in flipping all spins with zero local field, starting with the ground-state configuration. This allows to explore all states within a single-spin-flip cluster of ground-state configurations (see below). In Fig. 8 a typical evolution of the magnetization (scattered points) and its running average for $L=300$, $p=0.1$, averaged over 100 samples, are shown as a function of the number of Monte Carlo steps. We observe that after few hundred MC steps the simulation is equilibrated, i.e., the relative fluctuations of the average magnetization are less than 10^{-3}. Additionally, we see that the value of the magnetization found by the ground-state algorithm, i.e., for zero MC steps, is slightly outside the scattering of the datapoints for large Monte Carlo steps, and that the selected configuration has a lower magnetization value. To check whether this is a coincidence or not, we did some test by applying the matching algorithm to a mainly ferromagnetic system with some antiferromagnetics bond. Surprisingly, we found that that the free spins of the configuration are selected without preferential direction respect to the direction of the total magnetization. However there could be some bias for more complicated domain walls, but we cannot fully explain it since we used a commercial library. Besides, compared to the final statistical error bars (see below), this difference is negligible. Hence we conclude that the ground state obtained by the matching algorithm exhibits a typical magnetization of the cluster, in which the ground state is located.

Anyway, the set of ground states usually is divided into *several* clusters:[34] different ground states belong to the same cluster if they are related by a sequence of single free spin flips (i.e., spin in zero local field). Ground states in different cluster can only be reached from each other by making cooperative flips of multiple spins or when using single-spin flips via increasing the energy. This means that with our single-spin-flip MC algorithm at $T=0$ the system always stays in the same cluster. In principle one can enumerate all ground states.[33] Since the ground-state degeneracy grows exponentially fast with the system size, only small systems can be treated like this.

Thus, we have applied an alternative method to find different ground states, the so-called ϵ*-coupling method*. It allows us to obtain ground states from different clusters, but no exhaustive enumeration is necessary. The basic idea is to first add a perturbation to the system which tends to increase the energy if two neighboring spins are in the same relative orientation as in the ground state and then to recalculate the ground state. Let $S_i^{(1)}$ be the ground-state spin configuration. We then perturb the couplings J_{ij} by an amount proportional to $S_i^{(1)}S_j^{(1)}$ in order to repel the system from the ground state. This perturbation, which depends upon a positive parameter ϵ, is defined by

$$J_{ij}\rightarrow J_{ij}+\Delta J_{ij}, \tag{8}$$

where

$$\Delta J_{ij}=-\frac{\epsilon}{N_b}S_i^{(1)}S_j^{(1)}, \tag{9}$$

where N_b is the number of bonds in the system. We then recompute the ground state and check that the new configuration is still a ground state of the unperturbed Hamiltonian. This is our second ground state $S_i^{(2)}$. The next step, to obtain a third ground state, consists of adding a perturbation in order to repel the system from both ground states obtained so far. This process can be iterated. For a number n of steps of this process, we have

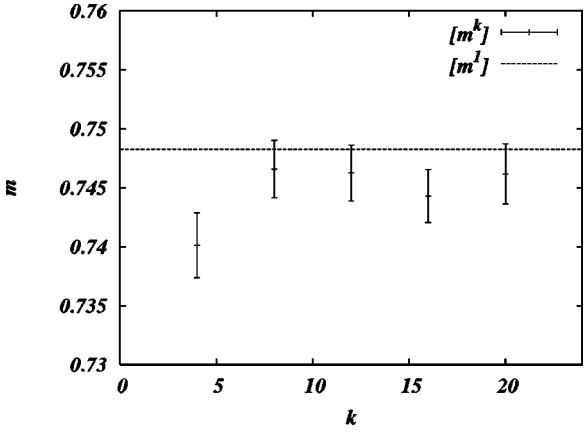

FIG. 9. Magnetization obtained after averaging over k independent ground states as a function of k. The horizontal lines indicate the magnetization of the first ground state $k=1$. The data is for $L=100$, $p=0.103$ and averaged over 1000 realizations.

$$\Delta J_{ij} = -\alpha \sum_{k=1}^{n} \frac{\epsilon}{N_b} S_i^{(k)} S_j^{(k)}, \tag{10}$$

where α is a scaling factor that we choose equal to 1. In this way we hope to find configurations belonging to different clusters, even if this procedure is not completely under control since it is a biased random sampling in the space of configurations. To test the behavior of our method, we have calculated for each step k of the ϵ-coupling approach the magnetization m^k of the kth ground state. Figure 9 shows the resulting behavior of $[m^k]$, $[\cdots]$ denoting the average over the first $k-1$ iterations of the ϵ-coupling method and over 1000 configurations of the disorder ($L=300$, $p=0.1$). We observe that, within the statistical error bars, the magnetization for the first ground state, indicated by the horizontal lines, agrees well with the value obtained after averaging over several different degenerate ground-state configurations. Note that for small k the difference is larger. This is due to the fact that the ϵ-coupling method repels each configuration from the previously obtained ground states. Hence, for small k it will move strongly away from the first ground state. With increasing number k of steps, the different ground states will be scattered around in configuration space. If the $k=1$ ground state is typical with respect to the magnetization, then the average will converge to the initial value again, which seems to be the case here. Note that we have also checked for the different iterations of the ϵ-coupling method that performing an additional $T=0$ MC simulation changes the obtained magnetization values again only slightly. Since the ϵ-coupling method strongly slows the simulations and the differences are negligible within statistical error bars, we have restricted the simulations to the immediately obtained ground states ($k=1$), i.e., without applying the ϵ-coupling method.

In Fig. 10 the Binder cumulant is shown as a function of the concentration of p for different sizes $L \leqslant 500$, where we have obtained data for all concentrations $p=0.1$, 0.101, …, 0.107. It intersects close to $p_c^1 \sim 0.103$ except for the largest size, where the statistics is not so good. Hence, we again conclude $p_c^1=0.103(1)$ which agrees well with what we have

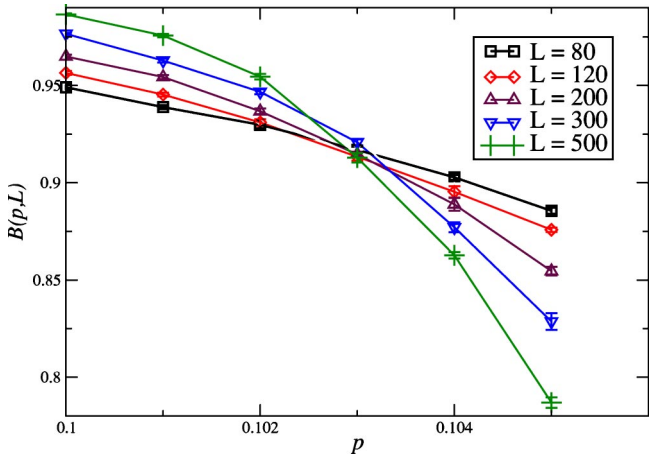

FIG. 10. Binder cumulant $B(p,L)=\frac{3}{2}(1-\langle m\rangle^4/3\langle m^2\rangle^2)$ as a function of the concentration of antiferromagnetic bonds p.

obtained above by studying domain wall energies. This also indicates that the matching algorithm indeed finds ground states which are typical with respect to the magnetization.

Finally, we present further ways to check the previous conclusions. We have performed another treatment of the data by trying to collapse all curves in Fig. 10 in a single one. This means we want to find the parameters which satisfy the finite-size scaling relation for the Binder cumulant:

$$B(p,L) = \tilde{B}(L^{1/\nu}(p - p_c)), \tag{11}$$

where ν is the critical exponent of the correlation length. We vary p_c and ν in order to minimize the functional $S(p_c,\nu)$. We find its minimum value for $p_c=0.103$ and $\upsilon=1.55(1)$($S \sim 2.2$), the resulting data collapse is illustrated in Fig. 11. The value for ν is consistent with the value $\nu=1.50(3)$ at the NP reported in Ref. 22, but differs from the value $\nu=1.33(3)$ found previously.[21] Since in the work of Merz and Chalker much larger system sizes are treated compared to the work of Honecker *et al.*, the value $\nu=1.50(3)$ appears more reliable. Hence, our result indicates that the transition at NP and at $T=0$ are in the same universality class.

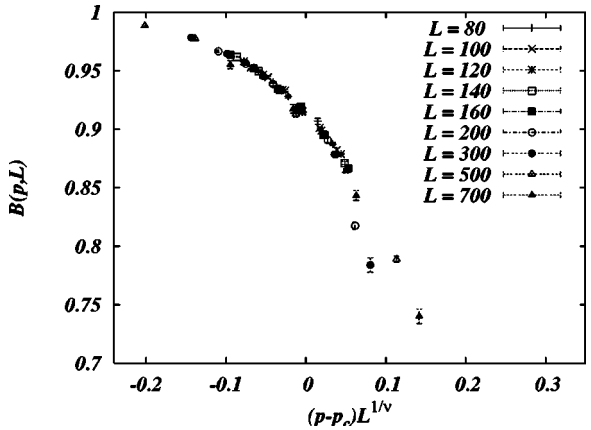

FIG. 11. Scaling plot of the Binder cumulant $B(p,L)$ as a function of $(p-p_c)L^{1/\nu}$ with $p_c=0.103$ and $\nu=1.55$.

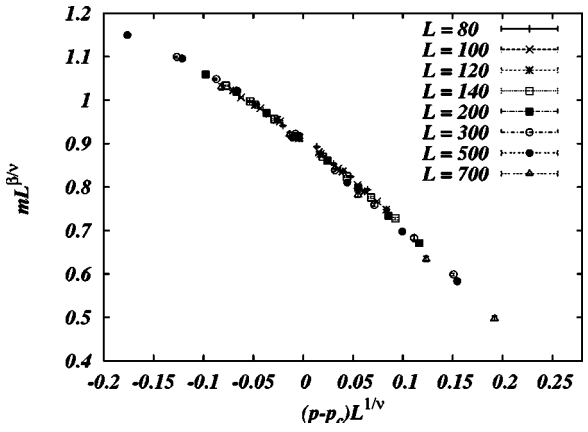

FIG. 12. Scaling plot of the rescaled magnetization $mL^{\beta/\nu}$ as a function of $(p-p_c)L^{1/\nu}$ with $p_c=0.103$, $\nu=1.55$, $\beta=0.9$.

Finally, we study the finite-size scaling behavior of the magnetization. The prediction for the magnetization is

$$m(p) = L^{-\beta/\nu}\tilde{m}((p-p_c)L^{1/\nu}), \tag{12}$$

where β is the critical exponent of the magnetization. Using $p_c=0.1032$, $\nu=1.55$, a good data collapse is obtained with $\beta=0.9(1)$, see Fig. 12.

V. CONCLUSIONS

To summarize, we have performed a systematic calculation of the domain-wall energy at zero temperature for the two-dimensional random-bond Ising model for different concentrations p of the antiferromagnetic bonds. By using a matching algorithm, we could study systems which are much larger than in previous studies.

We find that both ferromagnetic and spin-glass phases cease to exist at the same concentration $p_c=0.103(1)$. This means, we do not find any sign for an intermediate "random antiphase." Furthermore, the values of p_c at $T=0$ and at the Nishimori point, found in the most reliable studies so far,[21,22] are different, indicating a re-entrance of the paramagnetic phase.

Large system sizes $L \geqslant 500$ are needed to observe the true thermodynamic behavior with good accuracy. Slightly above p_c, the width of the distribution of domain-wall energies increases for small sizes, while it decreases for larger sizes. Note that in principle we cannot exclude that a similar turnover happens for smaller concentrations, e.g., $p=0.103$, at even larger system sizes $L>700$, which are out of reach of our algorithm. Nevertheless, this would mean that the real p_c is even smaller, hence the discrepancy between p_c and p_n would increase and the re-entrance became stronger.

ACKNOWLEDGMENTS

The authors have obtained financial support from the VolkswagenStiftung (Germany) within the program "Nachwuchsgruppen an Universitäten" and from the European Community via the Human Potential Program under Contract No. HPRN-CT-2002-00307 (DYGLAGEMEM), via the High-Level Scientific Conferences (HLSC) program, and via the Complex Systems Network of Excellence "Exystence." The simulations were performed at the Paderborn Center for Parallel Computing in Germany and on a workstation cluster at the Institut für Theoretische Physik, Universität Göttingen, Germany.

[1] Reviews on spin glasses can be found in K. Binder and A. P. Young, Rev. Mod. Phys. **58**, 801 (1986); M. Mezard, G. Parisi, and M. A. Virasoro, *Spin Glass Theory and Beyond* (World Scientific, Singapore, 1987); K. H. Fisher and J. A. Hertz, *Spin Glasses* (Cambridge University Press, Cambridge, 1991); *Spin Glasses and Random Fields*, edited by A. P. Young (World Scientific, Singapore, 1998).
[2] N. Kawashima and H. Rieger, Europhys. Lett. **39**, 85 (1997).
[3] H. Rieger, L. Santen, U. Blasum, M. Diehl, M. Jünger, and G. Rinaldi, J. Phys. A **29**, 3939 (1996).
[4] A. K. Hartmann and A. P. Young, Phys. Rev. B **64**, 180404 (2001).
[5] J. Houdayer, Eur. Phys. J. B **22**, 479 (2001).
[6] A. C. Carter, A. J. Bray, and M. A. Moore, Phys. Rev. Lett. **88**, 077201 (2002).
[7] W. L. McMillan, J. Phys. C **17**, 3179 (1984).
[8] A. J. Bray and M. A. Moore, in *Glassy Dynamics and Optimization*, edited by J. L. van Hemmen and I. Morgenstern (Springer, Berlin, 1986).
[9] D. S. Fisher and D. A. Huse, Phys. Rev. Lett. **56**, 1601 (1986); D. S. Fisher and D. A. Huse, Phys. Rev. B **38**, 386 (1988).
[10] A. J. Bray and M. A. Moore, J. Phys. C **14**, L463 (1984).
[11] A. K. Hartmann and M. A. Moore, Phys. Rev. Lett. **90**, 127201 (2003).
[12] F. Barahona, R. Maynard, R. Rammal, and J. P. Uhry, J. Phys. A **15**, 673 (1982).
[13] R. Maynard and R. Rammal, J. Phys. (France) Lett. **43**, L347 (1982).
[14] Y. Ozeki, J. Phys. Soc. Jpn. **59**, 3531 (1990).
[15] N. Kawashima and H. Rieger, Europhys. Lett. **39**, 85 (1997).
[16] H. Nishimori, J. Phys. Soc. Jpn. **55**, 3305 (1986).
[17] H. Kitatani, J. Phys. Soc. Jpn. **61**, 4049 (1992).
[18] A. K. Hartmann and H. Rieger, *Optimization Algorithms in Physics*, (Wiley-VCH, Berlin, 2001).
[19] H. Nishimori, Prog. Theor. Phys. **66**, 1169 (1981); **76**, 305 (1986).
[20] P. Le Doussal and A. B. Harris, Phys. Rev. Lett. **61**, 625 (1988).
[21] A. Honecker, M. Picco, and P. Pujol, Phys. Rev. Lett. **87**, 047201 (2001).
[22] F. Merz and J. T. Chalker, Phys. Rev. B **65**, 054425 (2002).
[23] I. Bieche, R. Maynard, R. Rammal, and J. P. Uhry, J. Phys. A **13**, 2553 (1980).
[24] F. Barahona, R. Maynard, R. Rammal, and J. P. Uhry, J. Phys. A **15**, 673 (1982).
[25] U. Derigs and A. Metz, Math. Program. **50**, 113 (1991).
[26] W. J. Cook, W. H. Cunningham, W. R. Pulleyblank, and A.

Schrijver, *Combinatorial Optimization* (Wiley, New York, 1998).
[27] B. Korte and J. Vygen, *Combinatorial Optimization - Theory and Algorithms* (Springer, Heidelberg, 2000).
[28] K. Mehlhorn and St. Näher, *The LEDA Platform of Combinatorial and Geometric Computing* (Cambridge University Press, Cambridge, 1999); see also http://www.algorithmic-solutions.de
[29] N. Kawashima and N. Ito, J. Phys. Soc. Jpn. **62**, 435 (1993).
[30] W. H. Press, S. A. Teukolsky, W. T. Vetterling, and B. P. Flannery, *Numerical Recipes in C* (Cambridge University Press, Cambridge, 1995).
[31] K. Binder, Z. Phys. B: Condens. Matter **43**, 119 (1981).
[32] R. N. Bhatt and A. P. Young, Phys. Rev. Lett. **54**, 924 (1985); Phys. Rev. B **37**, 5606 (1988).
[33] J. W. Landry and S. N. Coppersmith, Phys. Rev. B **65**, 134404 (2002).
[34] A. K. Hartmann, Phys. Rev. E **63**, 016106 (2001).